Supporting Information

Coumarin-based Fluorescent Probes for Super-resolution and Dynamic Tracking of Lipid Droplets

Hongkang Xu,[a] Huihui Zhang,[a] Gang Liu,[a] Lin Kong,[a] Xiaojiao Zhu,*[a] Xiaohe Tian,[b] Zhongping Zhang,[a] Ruilong zhang,[a] Zhichao Wu,[a] Yupeng Tian [a], Hongping Zhou,*[a]

[a] *College of Chemistry and Chemical Engineering, Anhui University and Key Labotatory of Functional Inorganic Materials Chemistry of Anhui Province, Anhui Province Key Laboratory of Chemistry for Inorganic/Organic Hybrid Functionalized Materials, 230601, Hefei, P.R. China.*

** Prof. Hongping Zhou, Email: zhpzhp@263.net*

[b] *School of Life Sciences, Anhui University, Hefei 230601, P. R. China.*

Experimental Section S-4
Scheme S1. Synthetic route for CM2P and CM4P S-4
Figure S1. ^{1}H NMR spectrum of CM2P (Acetone-d_6). S-7
Figure S2. ^{13}C NMR spectrum of CM2P (Acetone-d_6). S-7
Figure S3. ESI-Mass spectrum of CM2P S-8
Figure S4. ^{1}H NMR spectrum of CM4P (Acetone-d_6). S-8
Figure S5. ^{13}C NMR spectrum of CM4P (Acetone-d_6). S-9
Figure S6. ESI-Mass spectrum of CM4P. S-9
X-ray crystallography S-10
Figure S7. ORTEP diagram (with 50% thermal ellipsoid probability) structures of CM2P (a) and CM4P (b) S-10
Table S1. The crystallographic data of CM2P and CM4P. S-10
Photo-physical Properties S-11
Figure S8. UV-*vis* absorption and One-photon excited fluorescence spectra of CM2P (a and b) and CM4P (c and d) in different solvents. S-11
Figure S9. Time-resolved lifetime fluorescence curves of CM2P (a) and CM4P (b) in different solvents. S-11
Figure S10. Energy levels of the HOMO and LUMO, energy gaps and electron cloud distributions of CM2P (a) and CM4P (b) molecules calculated by the B3LYP/6-31G program S-11
Figure S11. Two-photon excited fluorescence spectra of CM2P in AcoEt (a), THF (b), DMF (c), MeCN (d) and DMSO (e) S-12
Figure S12. The verification of CM2P two-photon excited fluorescence in AcoEt (a), THF (b), DMF (c), MeCN (d) and DMSO (e) S-12
Figure S13. Two-photon excited fluorescence spectra of CM2P in AcoEt (a), THF (b), DMF (c), MeCN (d) and DMSO (e) S-13
Figure S14. The verification of CM4P two-photon excited fluorescence in AcoEt (a), THF (b), DMF (c), MeCN (d) and DMSO (e) S-13
Table S2. The photophysical properties of CM2P and CM4P S-14
Figure S15. One-photon fluorescence emission spectra of interaction between CM4P (10 μM in PBS buffer, pH = 7.4) with liposome, calf thymus DNA, RNA, bovine serum albumin (BSA), human serum albumin (HSA), adenosine triphosphate (ATP), adenosine diphosphate (ADP) and histone (200 μg/mL). S-15
Figure S16. One-photon fluorescence emission spectra of interaction between CM4P (10 μM in PBS buffer, pH = 7.4) with liposome (2 mM), O/W emulsions (2 mM). S-15
Figure S17. (a) Size intensity curves of CM2P (10 μM in PBS buffer, pH = 7.4), CM2P with liposome and just liposome (100 μg/mL). (b) Size intensity curves of CM4P (10 μM in PBS buffer, pH = 7.4), CM4P with liposome and just liposome (100 μg/mL) S-16
Figure S18. (a) Size intensity curves of CM2P (10 μM in PBS buffer, pH = 7.4), CM2P with O/W

emulsions (2 mM) and just O/W emulsions (2 mM). (b) Size intensity curves of CM4P (10 μM in PBS buffer, pH = 7.4), CM4P with O/W emulsions (2 mM) and just O/W emulsions (2 mM)..S-16
Figure S19. Cell viability of HeLa cells treated by CM2P (a) and CM4P (b) with different conditions (5, 10, 15, 20, 25 μM) for different time (12 h, 24 h and 36 h) (n = 5). Error bar represents standard deviation (SD).....S-17
Figure S20. Confocal fluorescence images of HeLa cells stained with CM2P and CM4P for different concentrations (2, 4, 6, 8, 10 μM). (Incubation time: 25 min, λ_{ex} = 405 nm, λ_{em} = 460-500 nm) Scale bar: 20 μm S-17
Figure S21. Co-localization images of live HeLa cells with CM4P (4 μM) and Cell-Mask Deep Red (a1-d1), ER-Tracker Red (a2-d2), Mito-Tracker Deep Red (a3-d3)，Lyso-Tracker Deep Red (a4-d4), HCS LipidTOX™ Deep Red (a5-d5), respectively. (a) Confocal fluorescence images of CM4P (a1-a5) (λ_{ex} = 400 nm, λ_{em} = 460-500 nm). (b) Confocal fluorescence images of Cell-Mask Deep Red, ER-Tracker Red, Mito-Tracker Deep Red, Lyso-Tracker Deep Red and HCS LipidTOX™ Deep Red, respectively. (c) The merged images of a and b, respectively. (d) Co-localization images. Scale bar: 20 μm.....S-18
Table S3. The co-localization study of CM2P and CM4P with various commercially available organelle-specific dyes.....S-19
Figure S22. Co-localization images of live HeLa cells with CM2P (10 μM) and HCS LipidTOX™ Deep Red. (a) Confocal fluorescence image of CM2P (λ_{ex} = 405 nm, λ_{em} = 460-500 nm). (b) Confocal fluorescence image of HCS LipidTOX™ Deep Red (λ_{ex} = 637 nm, λ_{em} = 645-675 nm). (c) The bright- field image. (d) Merged image of a and b. (e) Merged image of a-c. (f) The fluorescence profiles of CM2P and HCS LipidTOX™ Deep Red along the white line in d. Scale bar: 20 μm.....S-19
Figure S23. (a) Confocal fluorescence images of CM2P in fixed HeLa cells (4 μM, λ_{ex} = 405 nm, λ_{em} = 460-500 nm). (b) STED image of CM2P (4 μM, λ_{ex} = 405 nm, λ_{em} = 460-500 nm). (c) The intensity plot profile of a LD and the comparison of full width at half maximum (FWHM) from a and b S-20
Figure S24. (a) STED image of CM2P in live HeLa cells (4 μM, λ_{ex} = 405 nm, λ_{em} = 460-500 nm). (b) STED image of CM4P in live HeLa cells (4 μM, λex = 405 nm, λem = 460-500 nm). (c) Numbers of LDs from two observed cells. (d) Diameter distribution of LDs from two observed cells. Scale bar = 10 μm. Numbers and diameters of LDs were quantified by ImageJ software (version 1.48V).....S-21
References S-21

Experimental Section

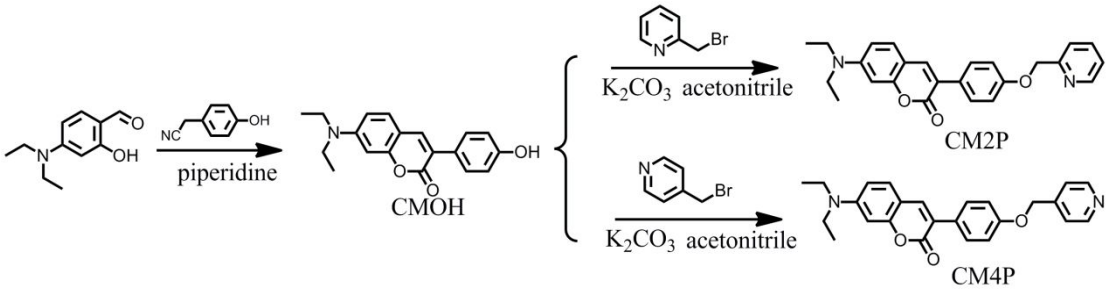

Scheme S1. Synthetic route for CM2P and CM4P.

1.1 Synthesis of CM2P and CM4P

Compounds were synthesized on the basis of CMOH showed in **Scheme S1**. CMOH was synthesized according to a reported method.[1]

CM2P: CMOH (2.00 g, 6.47 mmol) and 4 drops 18-C-6 were added to 30 mL acetonitrile of 2-bromomethyl pyridine hydrobromide (1.96 g, 7.76 mmol) and K_2CO_3 (2.76 g, 20.00 mmol), then the mixture was refluxed at 80 °C for 12 h. After the solvent was evaporated under reduced pressure and poured into 50 mL dichloromethane, the solid was removed by filtration. After the filtrate was evaporated under reduced pressure, the crude product was purified by silica gel column chromatography using petroleum ether: ethyl acetate = 5:1) as eluent to afford 2.35 g (5.87 mmol) of yellow powder. Yield: 90.7%. ^{1}H NMR: (400 MHz, Acetone-d_6), δ (ppm): 8.60-8.58 (d, J = 8.0 Hz, 1H), 7.90 (s, 1H), 7.85-7.81 (t, J = 16.0 Hz, 1H), 7.73-7.70 (d, J = 12.0 Hz, 2H), 7.58-7.56 (d, J = 8.0 Hz, 1H), 7.48-7.46 (d, J = 8.0 Hz, 1H), 7.34-7.30 (t, J = 16.0 Hz, 1H), 7.09-7.07 (d, J = 8.0 Hz, 2H), 6.76-6.73 (d, J = 12.0 Hz, 1H), 6.54 (s, 1H), 5.24 (s, 2H), 3.56-3.50 (q, 4H), 1.24-1.21 (t, J = 12.0 Hz, 6H). ^{13}C NMR: (100 MHz, Acetone-d_6), δ (ppm): 161.54, 159.08, 158.28, 157.04, 151.44, 150.08, 140.38, 137.58, 130.32, 130.11 129.85, 123.58, 122.21, 120.69, 115.27, 109.88, 97.37, 71.48, 45.26, 12.77. FTMS (ESI): m/z 400.1787 ([M+H]$^+$, calcd m/z 401.1849).

CM4P: The synthetic method is the same as CM2P, 2-bromomethyl pyridine hydrobromide is replaced by 4-bromomethyl pyridine hydrobromide. Yield: 93.0%. ^{1}H NMR: (400 MHz, Acetone-d_6), δ (ppm): 8.60-8.59 (d, J = 4.0 Hz, 2H), 7.90 (s, 1H), 7.73-7.71 (d, J = 8.0 Hz, 2H), 7.48-7.46 (t, J = 8.0 Hz, 3H), 7.09-7.06 (t, J = 12.0 Hz, 2H), 6.75-6.73 (d, J = 8.0 Hz, 1H), 6.53 (s, 1H), 5.26 (s, 2H), 3.55-3.50 (q, J = 20.0 Hz, 4H), 1.24-1.21 (t, J = 12.0 Hz, 6H). ^{13}C NMR: (100

MHz, Acetone-d_6), δ (ppm): 161.51, 158.86, 157.05, 151.47, 150.81, 147.27, 140.43, 130.35, 130.12 130.04, 122.49, 120.62, 115.27, 109.88, 97.37, 68.74, 45.27, 12.77. FTMS (ESI): m/z 400.1787 ($[M+H]^+$, calcd m/z 401.1847).

1.2 X-ray crystallography

Single-crystal X-ray crystallographic studies: Data were collected on a Bruker Smart APEX II diffractometer with a CCD area detector. Raw data collection and reduction were done using APEX2 software.[2] The structures were solved by direct methods and refined by full-matrix least-squares on F^2 using the SHELXTL software package. Non-hydrogen atoms were refined with anisotropic displacement parameters during the final cycles.

The single crystals of compounds CM2P (CCDC: 1587300) and CM4P (CCDC: 1810866) were obtained fortunately from ethyl alcohol solution and acetonitrile solution respectively. The dihedral angle between the coumarin ring (P1) and benzene ring (P2) in 3-position of the coumarin are 34.895° and 9.454° for CM2P and CM4P, respectively. The dihedral angle between the pyridyl ring (P3) and the benzene ring (P2) are 32.172° and 4.614° for CM2P and CM4P, respectively. So, the planarity of CM4P is better than that of CM2P. We found that in test the fluorescence of CM2P and CM4P in aqueous solution can be observed under ultraviolet light, which could be the fluorescence of nanoparticles in aqueous solution. On account of the good planarity of **C**M4P, it is easier to assemble into larger particles in aqueous solution thus lead to the fluorescence quenching degree of CM4P is higher than CM2P.

1.3 Two-photon absorption cross-section

Two-photon absorption cross-sections of CM2P, CM4P were obtained by the two-photon excited fluorescence (TPEF) method at femtosecond laser piles and a Ti: sapphire system (680-1080 nm, 80 MHz, 140 fs) as the light source. Effective two-photon absorption cross-section ($\sigma\Phi$) values were determined by the following equation:

$$\sigma\Phi = \sigma_{ref}\Phi_{ref}\frac{c_{ref}}{c}\frac{n_{ref}}{n}\frac{F}{F_{ref}}$$

The subscripts *ref* stands for the reference molecule (Fluorescein). Φ is the quantum yield, n is the refractive index, F is the integrated area under the corrected emission spectrum, c is the concentration of the solution in $mol \cdot L^{-1}$. The σ_{ref} value of reference was taken from the literature.[3]

The two-photon induced fluorescence spectra of the reference and sample emitted at the same excitation wavelength were determined.

1.4 Cytotoxicity test

The effects of CM2P and CM4P on viability of cells were carried out using the methylthiazolyldiphenyl-tetrazolium bromide (MTT) assay. Hela cells were trypsinized and plated to 70 % confluence in 96 well plates 24 h before treatment. Prior to the compounds' treatment, the DMEM was removed and replaced with fresh DMEM, and aliquots of the CM2P, CM4P stock solutions were diluted to obtain the final concentrations of 5, 10, 15, 20, 25 μM. The treated cells were then incubated at 37 °C in 5% CO_2 for 12, 24, 36 h. Subsequently, the cells were treated with 5 mg/mL MTT (10 μL per well) and incubated for an additional 4 h (37 °C, 5 % CO_2). Then, DMEM was removed, the formazan crystals were dissolved in DMSO (100 μL per well), and the absorbance at 490 nm using a microplate reader (SpectraMax Paradigm). The absorbance measured for an untreated cell population under the same experimental conditions was used as the reference point to establish 100% cell viability. Duplicated experiments have been tested.

1.5 Preparation of liposomes and O/W emulsions

liposomes: Phosphatidyl choline (75.8 mg) was dissolved in 20 mL chloroform. After the solvent was evaporated under reduced pressure at 37℃, then 50 mL PBS buffer solution was added, the mixed solution was stirred with magnetic stirring or ultrasonic oscillation at room temperature for 2 h.

O/W emulsions： Glycerol trioleat (63.9 mg) was added to 50 mL PBS buffer solution containing 0.0025 mM hexadecyl trimethyl ammonium bromide as emulsifier to stabilize the O/W emulsion， the mixed solution was stirred with magnetic stirring or ultrasonic oscillation at room temperature for 6 h.

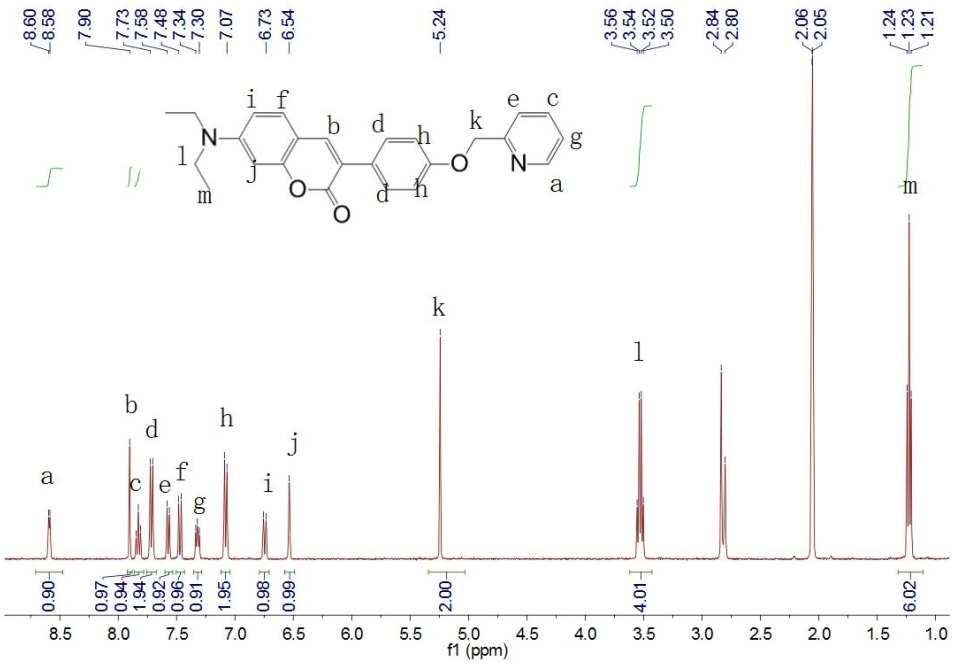

Figure S1. ^{1}H NMR spectrum of CM2P (Acetone-d_6)

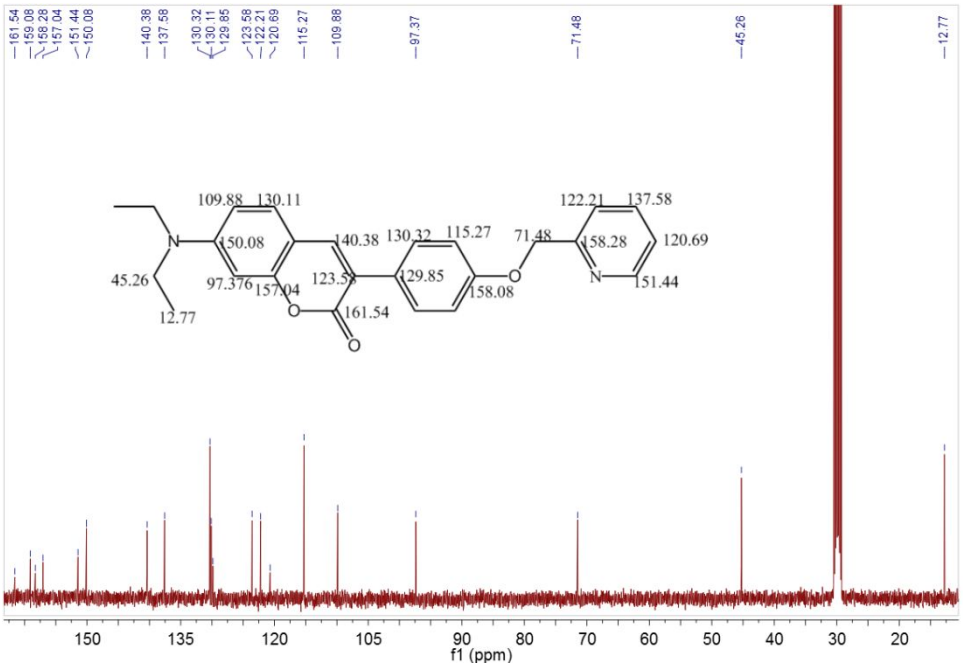

Figure S2. ^{13}C NMR spectrum of CM2P (Acetone-d_6)

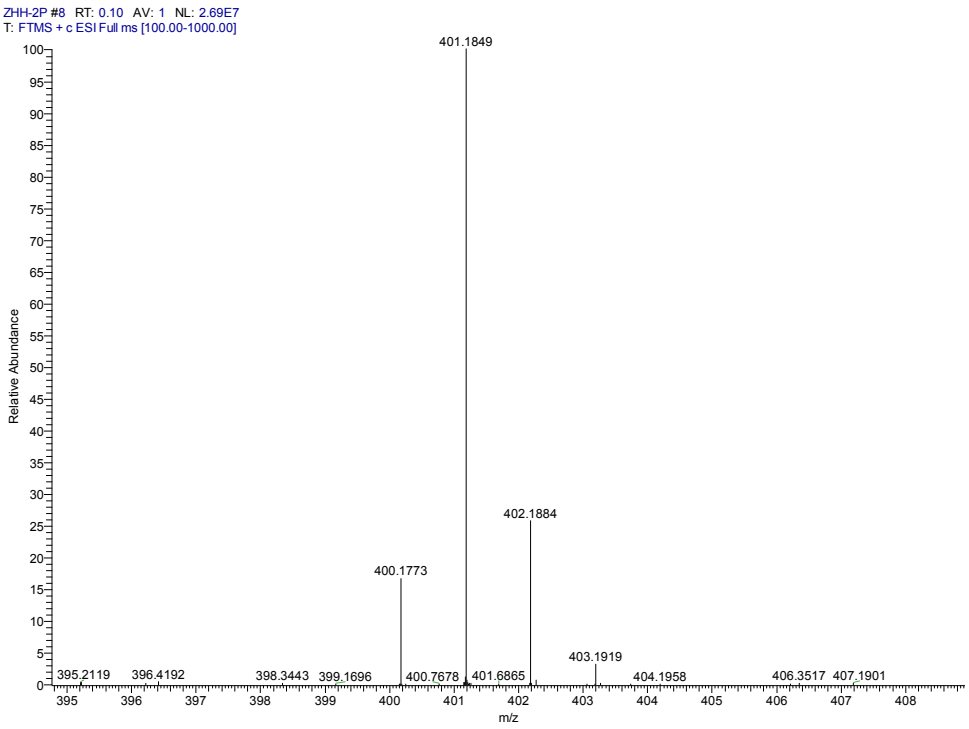

Figure S3. ESI-Mass spectrum of CM2P

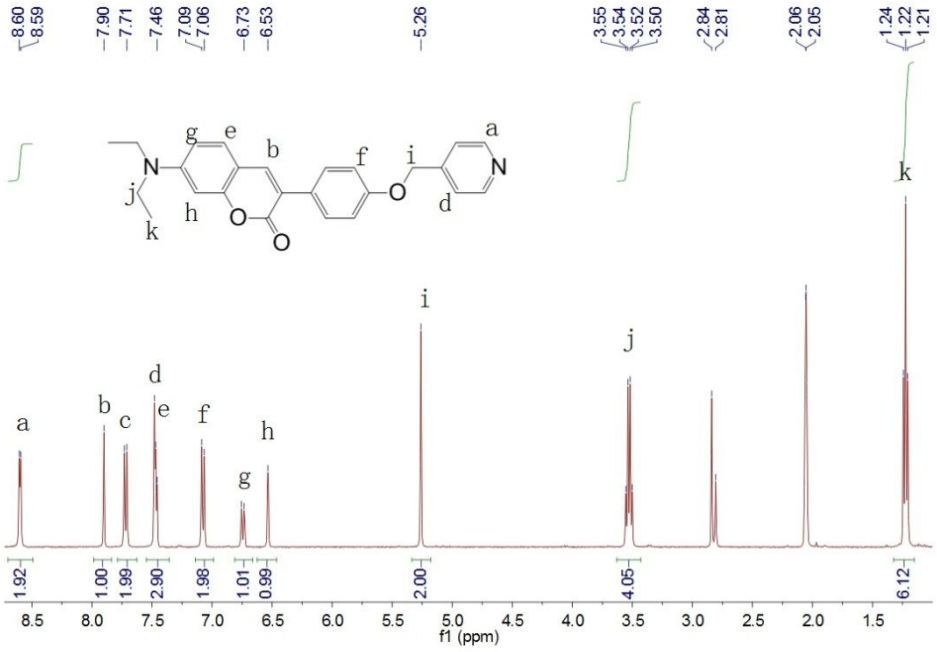

Figure S4. ^{1}H NMR spectrum of CM4P (Acetone-d_6)

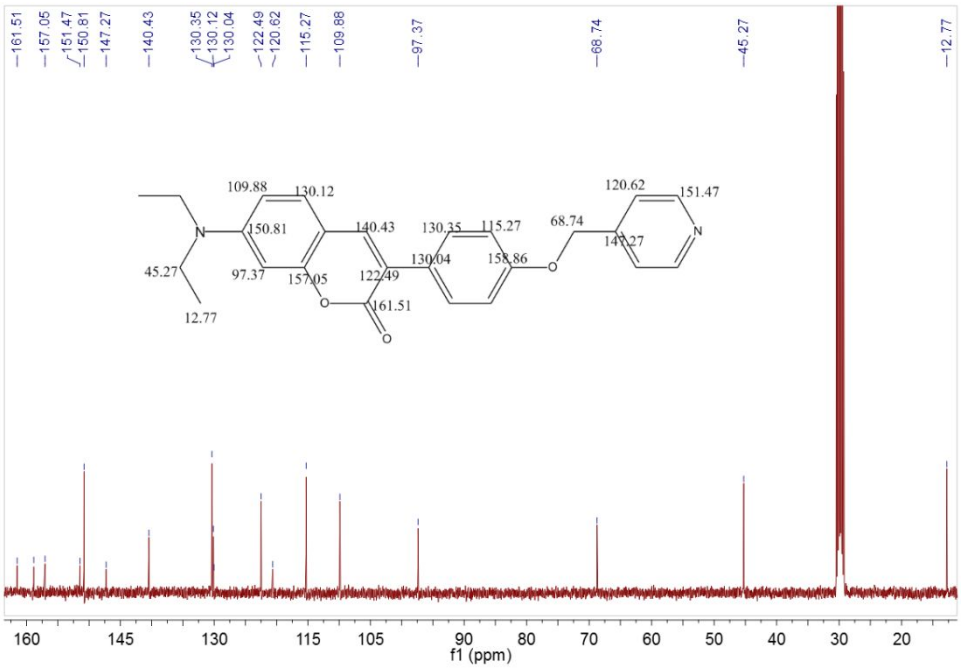

Figure S5. ^{13}C NMR spectrum of CM4P (Acetone-d_6)

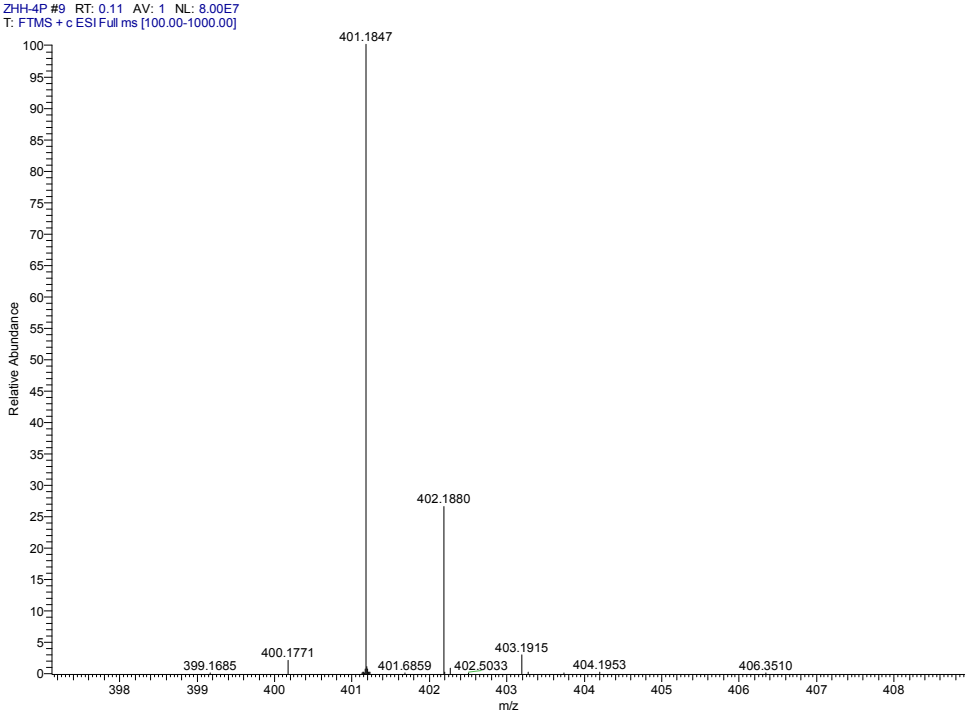

Figure S6. ESI-Mass spectrum of CM4P

X-ray crystallography

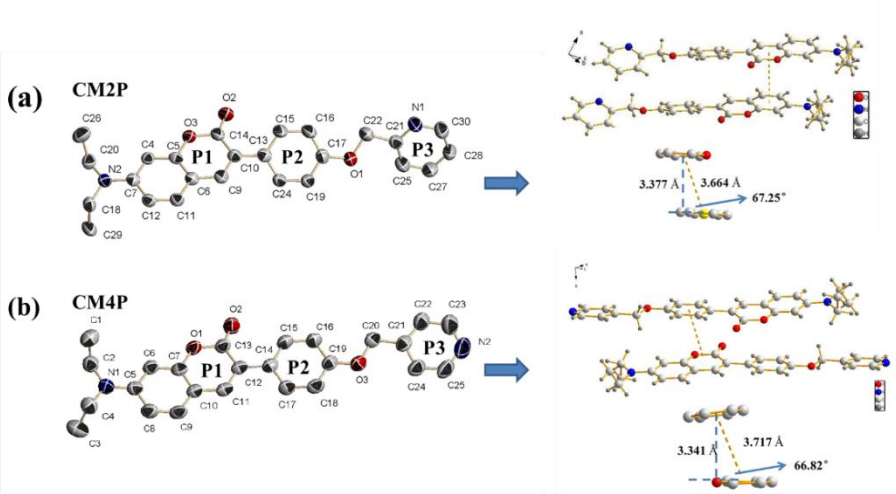

Figure S7. ORTEP diagram (with 50% thermal ellipsoid probability) structures of CM2P (a) and CM4P (b).

Table S1. Crystallographic data of CM2P and CM4P.

	CM2P	**CM4P**
Empirical formula	$C_{25}H_{24}N_2O_3$	$C_{25}H_{24}N_2O_3$
Formula weight	400.46	400.46
Crystal system	Monoclinic	Monoclinic
Space group	*P*2(1)/c	*P*2(1)/c
a[Å]	4.6245 (16)	17.070 (5)
b[Å]	14.020 (5)	15.438 (5)
c[Å]	32.033 (11)	8.000 (3)
α[°]	/	/
β[°]	91.558 (4)	100.202 (4)
γ[°]	/	/
V[Å^3]	2076.0 (12)	2074.9 (12)
Z	4	4
T[K]	296	296
D_{calcd}[g·cm^{-1}]	1.281	1.205
F(000)	848.0	848.0
μ[mm^{-1}]	0.09	0.09
R_{int}	0.035	0.027
R_1	0.0964	0.054
wR_2	0.249	0.184
GOF	0.98	0.96

Photo-physical Properties

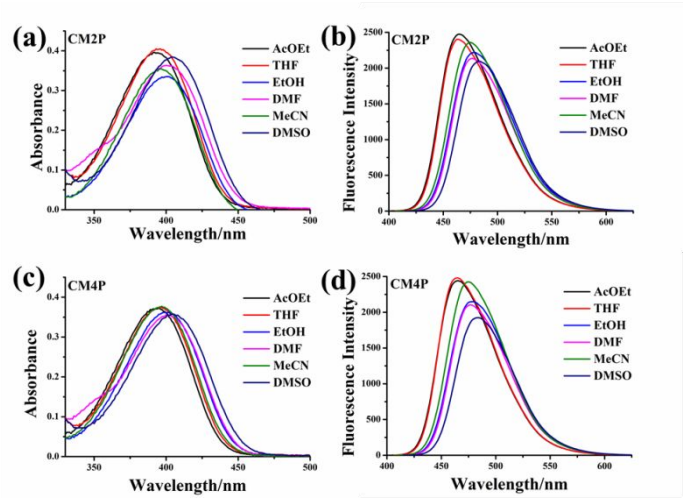

Figure S8. UV-*vis* absorption spectra and One-photon excited fluorescence spectra of CM2P (a and b) and CM4P (c and d) in different solvents.

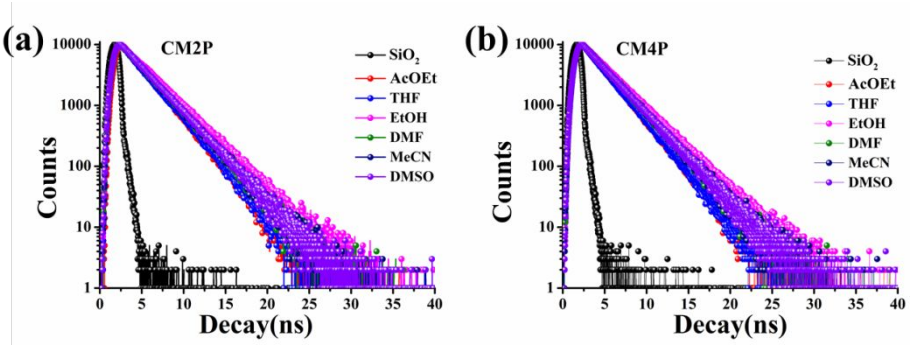

Figure S9. Time-resolved lifetime fluorescence curves of CM2P (a) and CM4P (b) in different solvents.

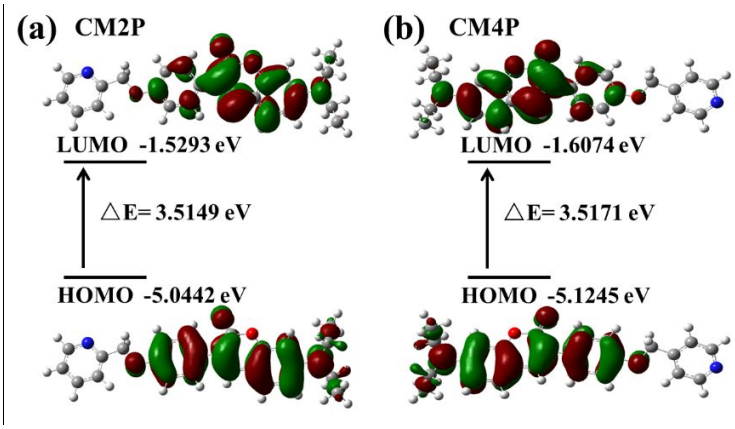

Figure S10. Energy levels of the HOMO and LUMO, energy gaps and electron cloud distributions of CM2P (a) and CM4P (b) molecules calculated by the B3LYP/6-31G program

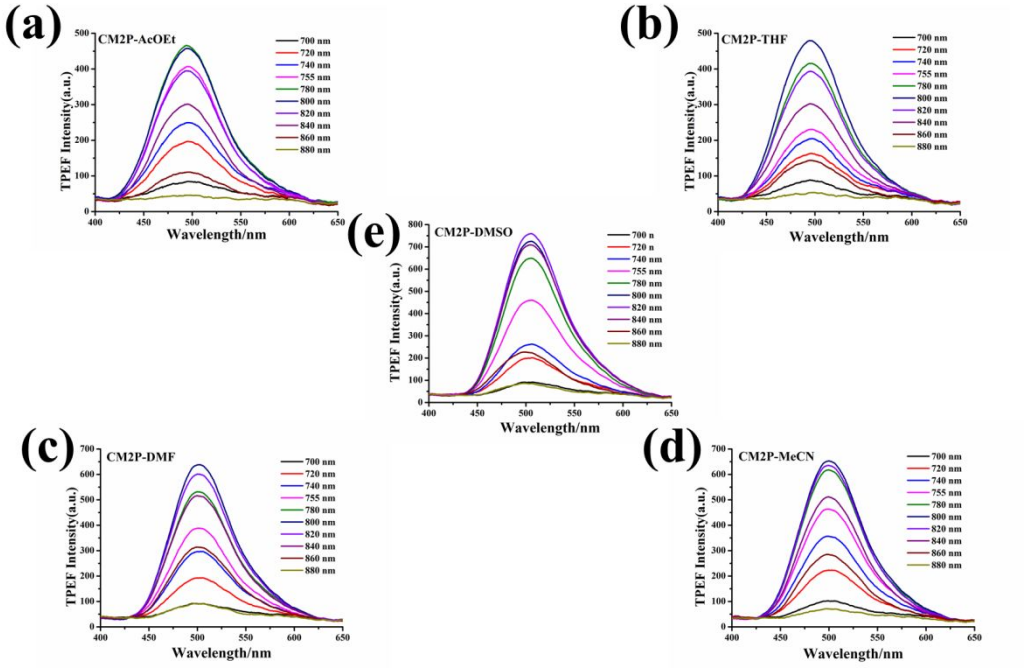

Figure S11. Two-photon excited fluorescence spectra of CM2P in AcoEt (a), THF (b), DMF (c), MeCN (d) and DMSO (e).

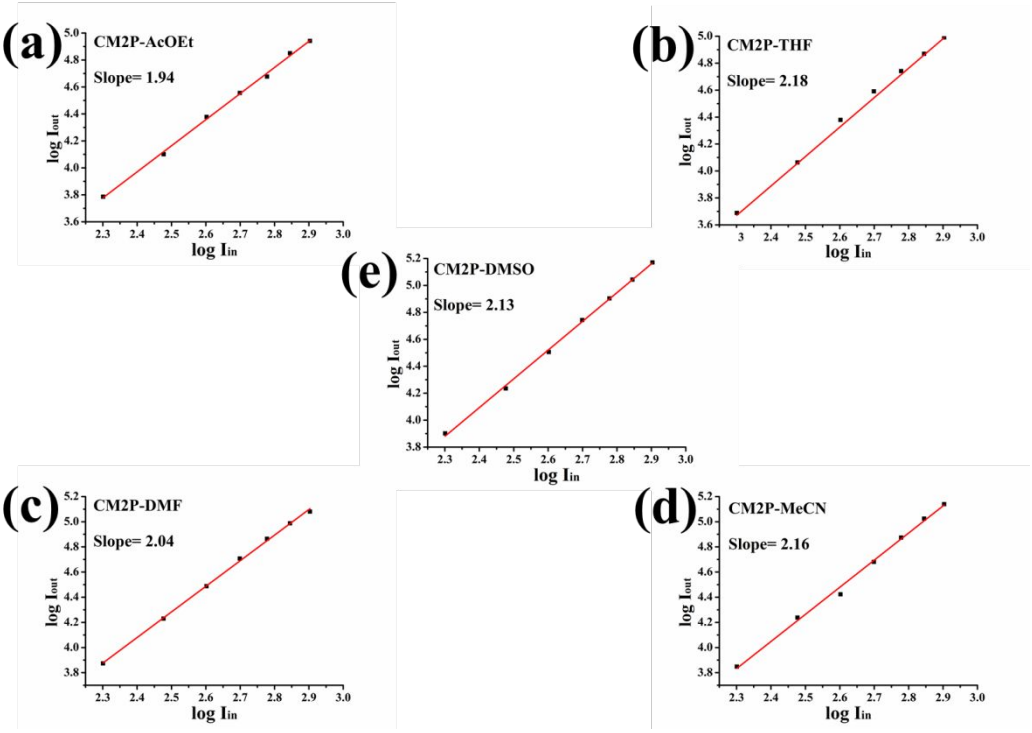

Figure S12. The verification of CM2P two-photon excited fluorescence in AcoEt (a), THF (b), DMF (c), MeCN (d) and DMSO (e).

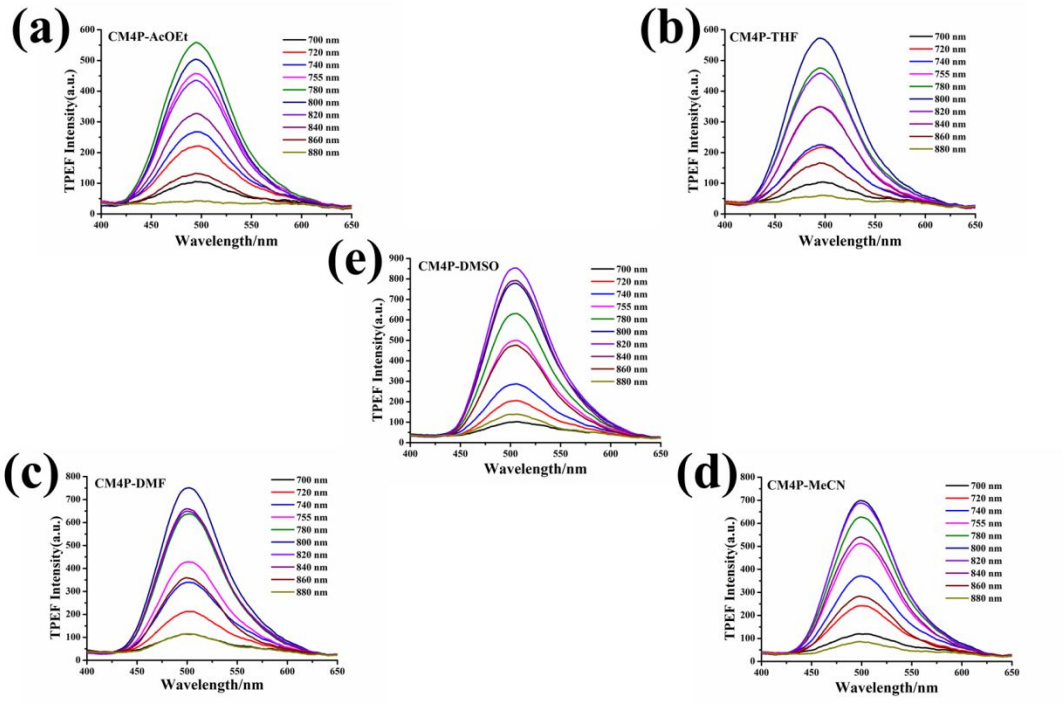

Figure S13. Two-photon excited fluorescence spectra of CM4P in AcoEt (a), THF (b), DMF (c), MeCN (d) and DMSO (e).

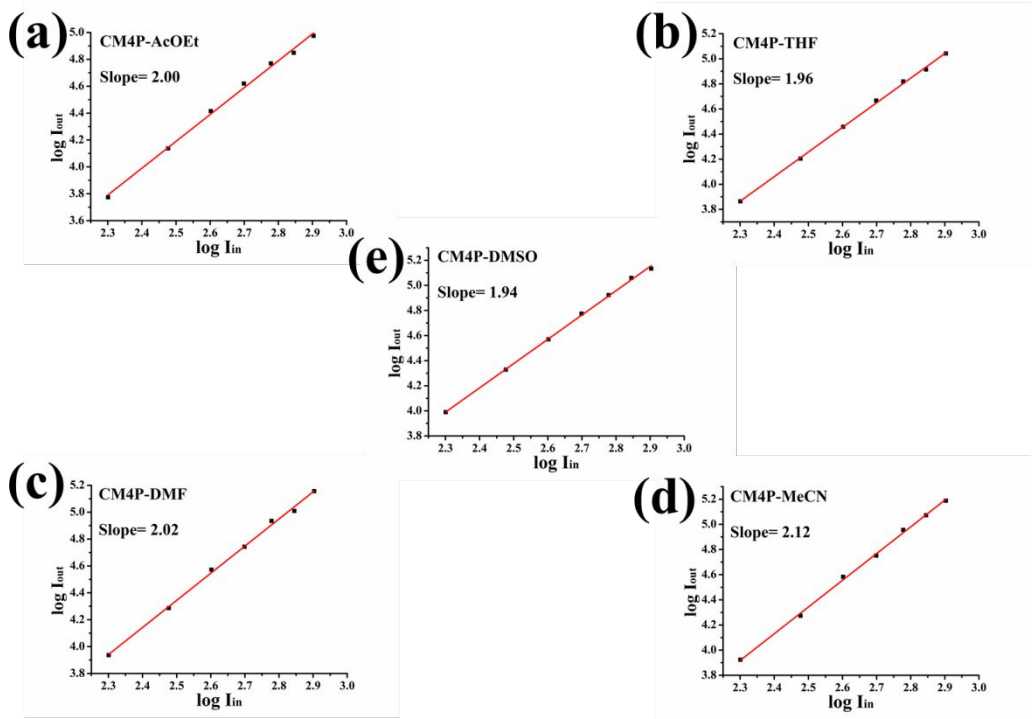

Figure S14. The verification of CM4P two-photon excited fluorescence in AcoEt (a), THF (b), DMF (c), MeCN (d) and DMSO (e).

Table S2. The photophysical properties of CM2P and CM4P

	solvents	λ_{abs}[a] (nm)	λ_{em}[b] (nm)	λ_{exc}[c] (nm)	λ_{max}[d] (nm)	ε[e] (10^4 $M^{-1}cm^{-1}$)	τ[f] (ns)	Φ[g]	$\Phi\sigma_{max}$[h]/ GM
CM2P	AcOEt	392	465	780	494	3.95	2.56	0.88	138
	THF	396	463	800	495	4.05	2.52	0.81	117
	EtOH	401	479	/	/	3.35	1.25	0.86	/
	DMF	400	477	800	501	3.63	2.73	0.83	146
	MeCN	396	475	800	500	3.55	2.82	0.82	172
	DMSO	404	483	820	504	3.85	2.90	0.82	177
CM4P	AcOEt	395	465	780	495	3.73	2.50	0.89	157
	THF	396	465	800	495	3.74	2.53	0.78	132
	EtOH	399	480	/	/	3.62	3.06	0.86	/
	DMF	400	477	800	500	3.56	2.82	0.83	177
	MeCN	397	475	800	499	3.77	2.80	0.81	174
	DMSO	405	484	820	504	3.58	2.87	0.80	191

[a] Absorption peak position in nm (1×10^{-5} mol/L). [b] Peak position of OPEF in nm, excited at the absorption maximum. [c] Maximum excitation wavelength in nm (1×10^{-4} mol/L). [d] TPEF peak position in nm pumped by femtosecond laser pulses at 500 mw at their maximum excitation wavelength. [e] ε is the molar absorptivity. [f] Fluorescence decay lifetime (ns), [g] Quantum yields determined by fully functional steady transient fluorescence spectrometer. [h] Effective two-photon absorption cross-sections determined using Fluorescein as the standard at 800 nm.

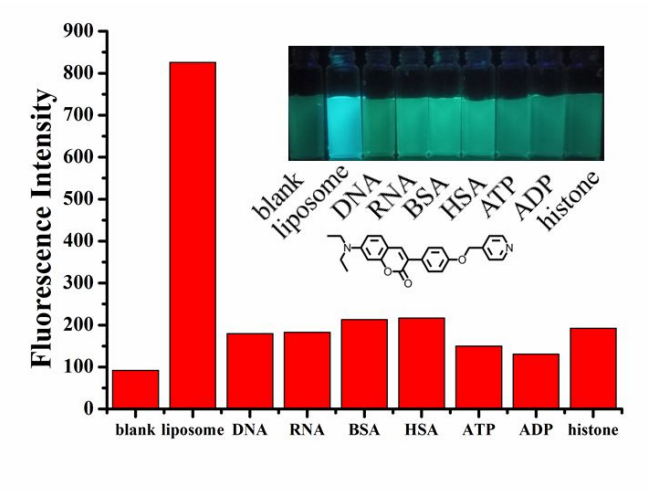

Figure S15. Fluorescence intensity of CM4P (10 μM in PBS buffer, pH = 7.4) with liposome, calf thymus DNA, RNA, bovine serum albumin (BSA), human serum albumin (HSA), adenosine triphosphate (ATP), adenosine diphosphate (ADP) and histone (200 μg/mL), respectively.

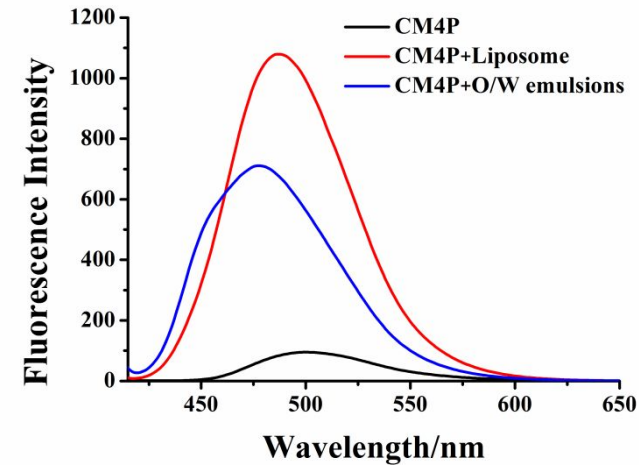

Figure S16. One-photon fluorescence emission spectra of CM4P (10 μM in PBS buffer, pH = 7.4) with liposome (2 mM), O/W emulsions (2 mM).

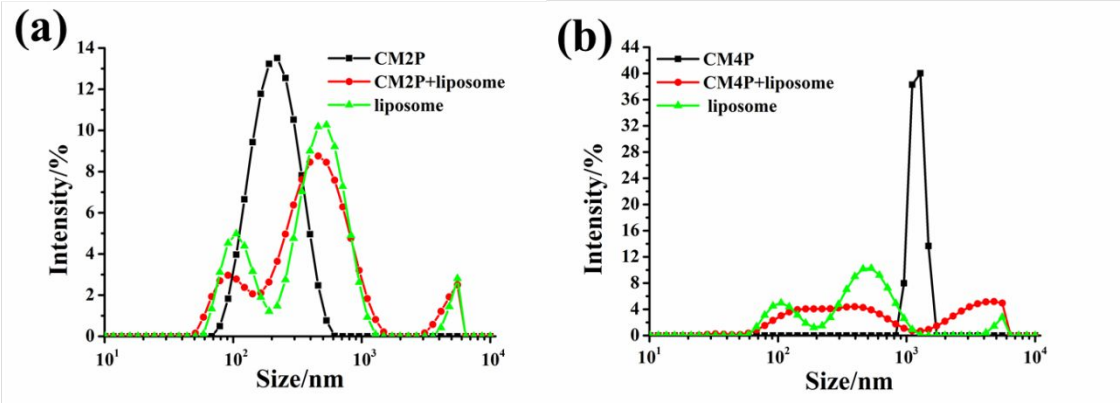

Figure S17. (a) Size intensity curves of CM2P (10 μM in PBS buffer, pH = 7.4), CM2P with liposome and just liposome. (b) Size intensity curves of CM4P (10 μM in PBS buffer, pH = 7.4), CM4P with liposome and just liposome (100 μg/mL).

In CM4P PBS buffer, the fluorescence was quenched due to the abrupt agglomeration of CM4P molecules into nanoparticles with the size range 800-1100 nm, which was verified by the DLS results (**Figure S17**). However, after adding liposome into CM4P PBS buffer, the lipophilic coumarin-based CM4P tend to permeate into the liposome with bi-layered enclosed vesicles structure, during which the interaction between lipophilic CM4P and liposome would break the agglomeration of CM4P and recover "turn-on" fluorescence and recover "turn-on" fluorescence. Similarly, the same phenomenon can also be observed for O/W emulsions verified by DLS results (**Figure S18**).

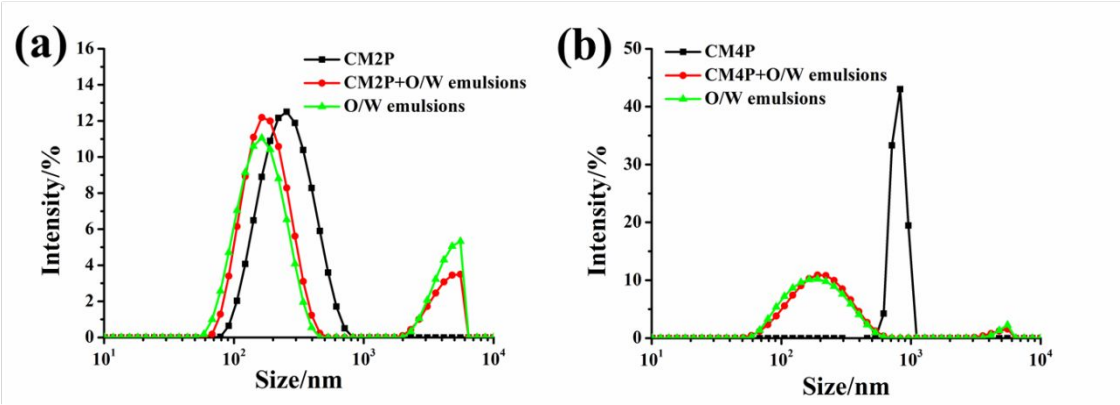

Figure S18. (a) Size intensity curves of CM2P (10 μM in PBS buffer, pH = 7.4), CM2P with O/W emulsions (2 mM) and just O/W emulsions (2 mM). (b) Size intensity curves of CM4P (10 μM in PBS buffer, pH = 7.4), CM4P with O/W emulsions (2 mM) and just O/W emulsions (2 mM).

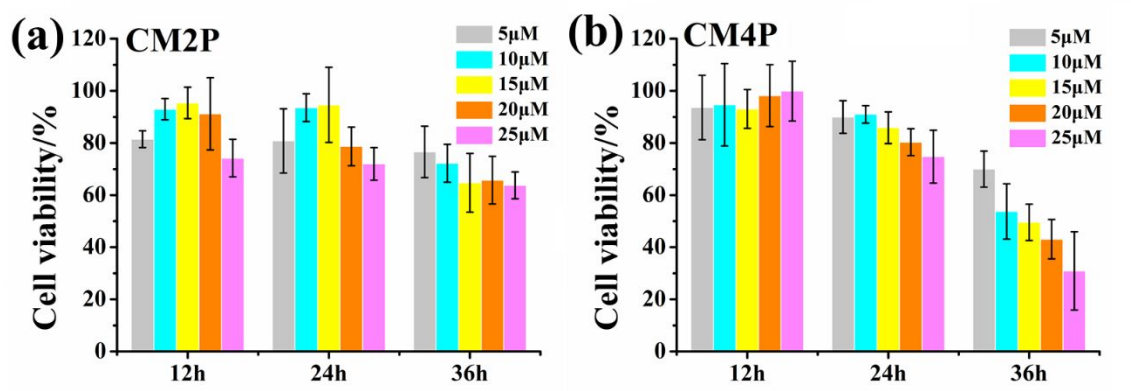

Figure S19. Cell viability of HeLa cells treated by CM2P (a) and CM4P (b) with different conditions (5, 10, 15, 20, 25 μM) for different time (12 h, 24 h and 36 h) (n = 5). Error bar represents standard deviation (SD).

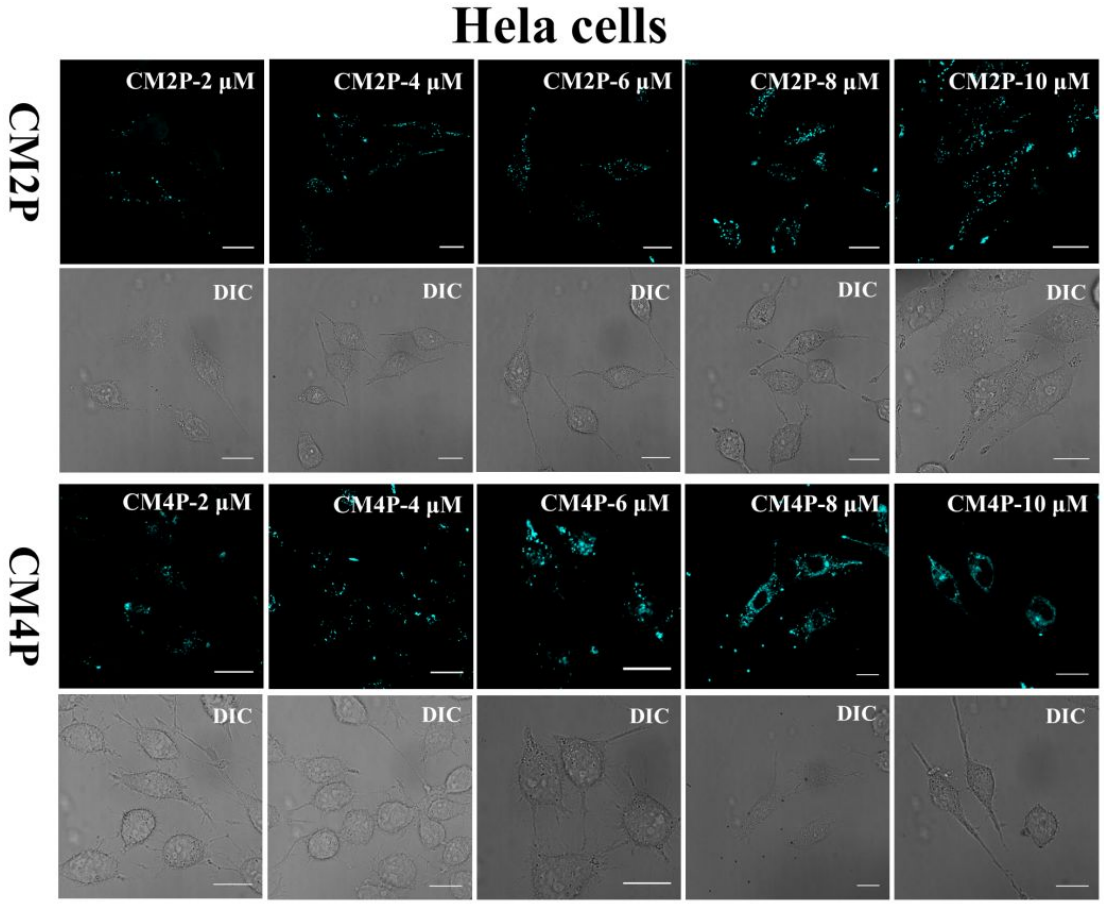

Figure S20. Confocal fluorescence images of HeLa cells stained with CM2P and CM4P for different concentrations (2, 4, 6, 8, 10 μM). (Incubation time: 25 min, λ_{ex} = 405 nm, λ_{em} = 460-500 nm) Scale bar: 20 μm.

As shown in **Figure S20**, with the increment of the staining concentrations, CM2P could well stain in the cytosol region with a specific pattern and emitted a brighter fluorescence when the concentration were 10 μM, whereas the CM4P show better results only when the concentration was no more than 4 μM. The co-localization study of CM4P (4 μM) with various commercially available organelle-specific dyes in living Hela cells are as shown in the **Figure S21** and **Table S3**. Although CM4P showed selectivity for LDs, the Pearson coefficient of CM4P and LD marker (HCS LipidTOX™ Deep Red) was not as high as that of CM2P and LD marker.

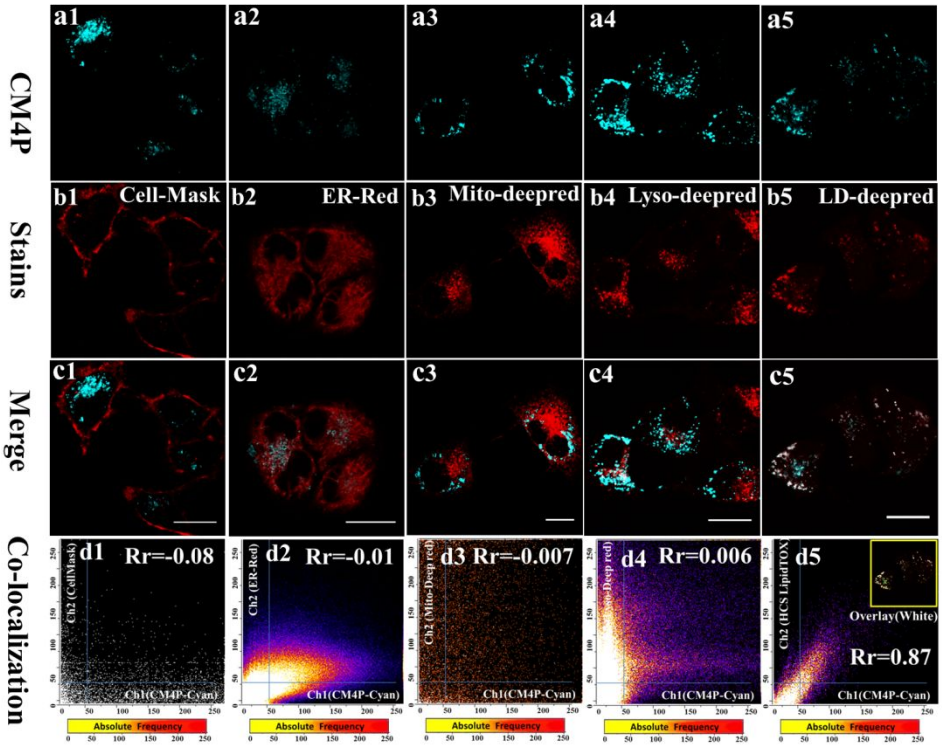

Figure S21. Co-localization images of live HeLa cells with CM4P (4 μM) and Cell-Mask Deep Red (a1-d1), ER-Tracker Red (a2-d2), Mito-Tracker Deep Red (a3-d3), Lyso-Tracker Deep Red (a4-d4), HCS LipidTOX™ Deep Red (a5-d5), respectively. (a) Confocal fluorescence images of CM4P (a1-a5) (λ_{ex} = 400 nm, λ_{em} = 460-500 nm). (b) Confocal fluorescence images of Cell-Mask Deep Red, ER-Tracker Red, Mito-Tracker Deep Red, Lyso-Tracker Deep Red and HCS LipidTOX™ Deep Red, respectively. (c) The merged images of a and b, respectively. (d) Co-localization images. Scale bar: 20 μm.

Table S3. The co-localization study of CM2P and CM4P with various commercially available organelle-specific dyes

Sample \ Commercial Dyes / Pearson coefficients	Cell-Mask Deep Red	ER-Tracker Red	Mito-Tracker Deep Red	Lyso-Tracker Deep Red	HCS LipidTOX™ Deep Red
CM2P	0.06	-0.004	-0.07	-0.03	0.92
CM4P	-0.08	-0.01	-0.007	0.006	0.87

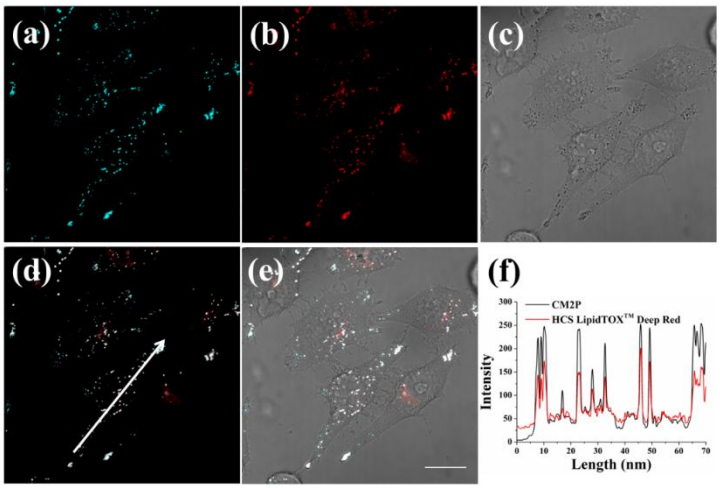

Figure 22. Co-localization images of live HeLa cells with CM2P (10 μM) and HCS LipidTOX™ Deep Red. (a) Confocal fluorescence image of CM2P (λ_{ex} = 405 nm, λ_{em} = 460-500 nm). (b) Confocal fluorescence image of HCS LipidTOX™ Deep Red (λ_{ex} = 637 nm, λ_{em} = 645-675 nm). (c) The bright-field image. (d) Merged image of a and b. (e) Merged image of a-c. (f) The fluorescence profiles of CM2P and HCS LipidTOX™ Deep Red along the white line in d. Scale bar: 20 μm.

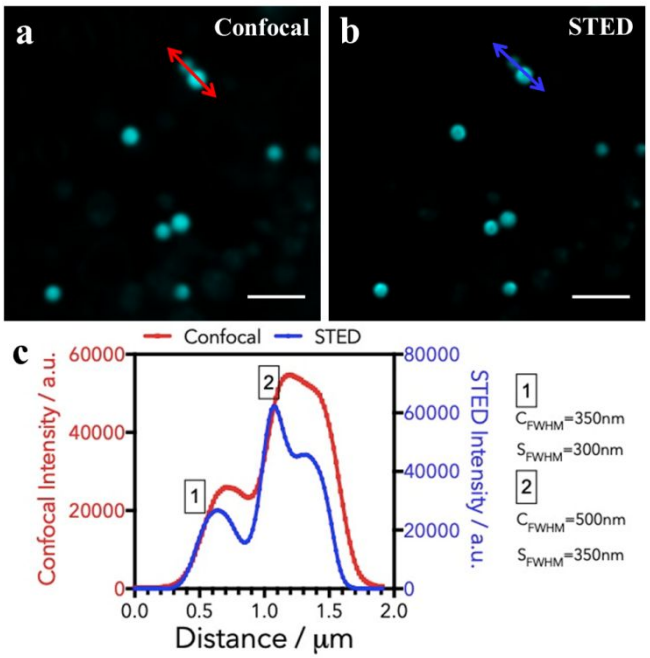

Figure S23. (a) Confocal fluorescence image of CM2P in fixed HeLa cells (4 μM, λ_{ex} = 405 nm, λ_{em} = 460-500 nm). (b) STED image of CM2P (4 μM, λ_{ex} = 405 nm, λ_{em} = 460-500 nm). (c) The intensity plot profile of two LDs marked by arrows from a and b, the comparison of full width at half maximum (FWHM) (blue for STED image and red for confocal fluorescence image). Scale bar = 2 μm.

The resolution of bio-imaging of fixed cell under conventional confocal imaging (Figure S23a) is inferior to that of the STED (Figure S23b). To quantitatively illustrate the resolution discrepancy, the intensity plot profiles of two LDs marked by arrows (blue for STED imaging and red for Confocal imaging) in corresponding images was displayed in Figure S23c, and the full width at half maximum (FWHM) of two peaks are summarized.

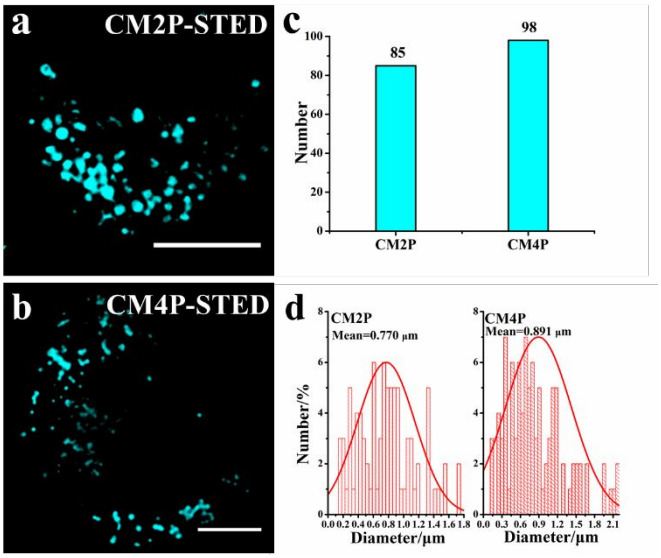

Figure S24. (a) STED image of CM2P in live HeLa cells (4 μM, λex = 405 nm, λem = 460-500 nm). (b) STED image of CM4P in live HeLa cells (4 μM, λex = 405 nm, λem = 460-500 nm). (c) Numbers of LDs from two observed cells. (d) Diameter distribution of LDs from two observed cells. Scale bar = 10 μm. Numbers and diameters of LDs were quantified by ImageJ software (version 1.48V)

The amount and diameter distribution of the captured LDs stained by CM4P are 98 and 890 ± 520 nm (**Figure S24**).

References

1. Yu, T.; Meng, J.; Zhang, P.; Zhao, Y.; Zhang, H.; Fan, D.; Chen, L.; Qiu, Y., Synthesis, crystal structures and photoluminescence of 7-(N,N'-diethylamino)-3-phenylcoumarin derivatives. *Spectrochim. Acta Part A Mol. Biomol. Spectrosc.* **2010**, 75 (3), 1036-1042.

2. Sheldrick, G., A short history of SHELX. *Acta Cryst.* **2008**, 64 (1), 112-122.

3. Makarov, N. S.; Drobizhev, M.; Rebane, A., Two-photon absorption standards in the 550-1600 nm excitation wavelength range. *Opt. Express* **2008**, 16 (6), 4029-4047.